ISCI, Volume *9*

Supplemental Information

AMP-Activated Protein Kinase Is Essential for the Maintenance of Energy Levels during Synaptic Activation

Claudia Marinangeli, Sébastien Didier, Tariq Ahmed, Raphaelle Caillerez, Manon Domise, Charlotte Laloux, Séverine Bégard, Sébastien Carrier, Morvane Colin, Philippe Marchetti, Bart Ghesquière, Detlef Balschun, Luc Buée, Jérôme Kluza, and Valérie Vingtdeux

Supplemental Figures

Figure S1

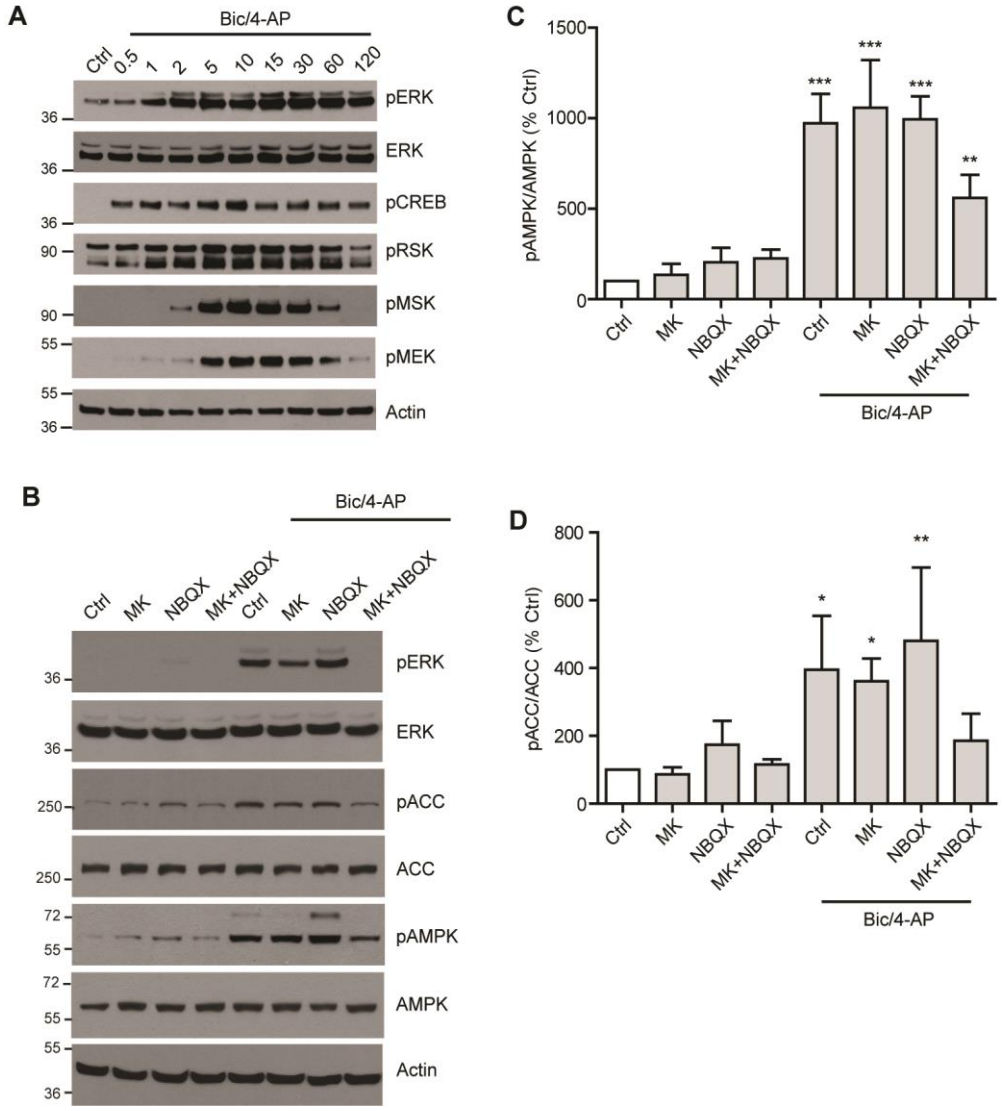

Figure S1 - AMPK activation following SA is dependent on NMDA and AMPA receptors activation. Related to Figure 1.

(**A**) Primary neurons were treated with Bic/4-AP for the indicated times and the activation of the MAPK pathway was monitored by immunoblotting with anti- phosphorylated ERK, CREB, RSK, MSK, MEK and total ERK and Actin antibodies. Results are representative of at least 3 experiments. (**B**) Primary neurons were pre-treated for 20 min with the NMDA receptors and AMPA receptors antagonists MK-801 (25 µM) and NBQX (20 µM), respectively. After pre-treatment, neurons were stimulated with Bic/4-AP for 10 min.

Activation of ERK and AMPK were monitored by immunoblotting with anti- phosphorylated ERK and total ERK and anti- phosphorylated AMPK and ACC, total AMPK, ACC, and Actin antibodies. Results are representative of at least 5 experiments. (**C-D**) Quantifications of WB as shown in B displaying the ratios phosphorylated AMPK/total AMPK (pAMPK/AMPK) and phosphorylated ACC/total ACC (pACC/ACC) expressed as percentage of control (n=3-5).

Results show mean ± SD. One-way ANOVA followed by Bonferroni's post-test was used for evaluation of statistical significance. * $p < 0.05$, ** $p < 0.01$, *** $p < 0.001$.

Figure S2

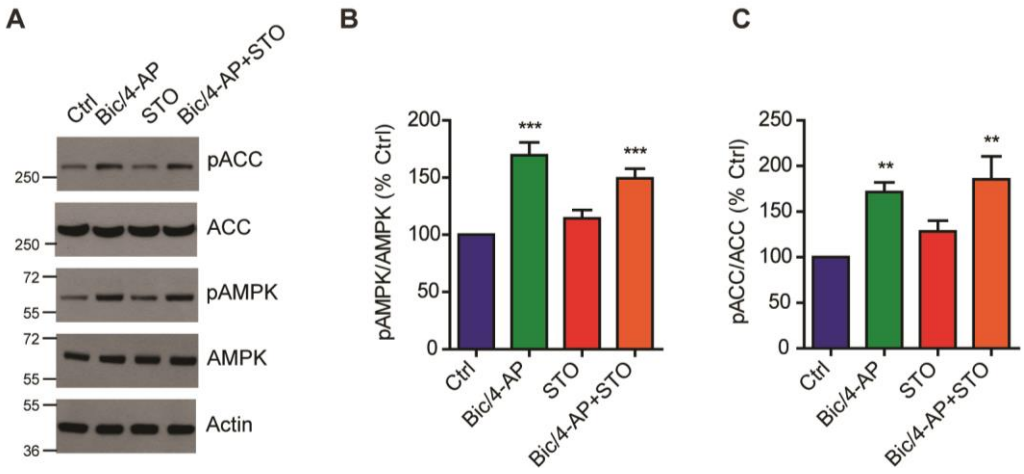

Figure S2 - SA induced activation of AMPK is not mediated by CaMKKβ. Related to Figure 1.

(**A**) Primary neurons treated with Bic/4-AP (10 min) after 20 min pre-treatment or not with the CaMKKβ specific inhibitor STO-609 (STO, 10 µM) were subjected to immunoblotting with anti- phosphorylated AMPK and ACC, total AMPK and ACC, and Actin. Results are representative of at least 5 experiments. (**B-C**) Quantifications of WB as in A showing the ratios phosphorylated AMPK/total AMPK (pAMPK/AMPK) and phosphorylated ACC/total ACC (pACC/ACC) expressed as percentage of control (n=5).

Results show mean ± SD. One-way ANOVA followed by Bonferroni's post-test was used for evaluation of statistical significance. * $p < 0.05$, ** $p < 0.01$, *** $p < 0.001$.

Figure S3

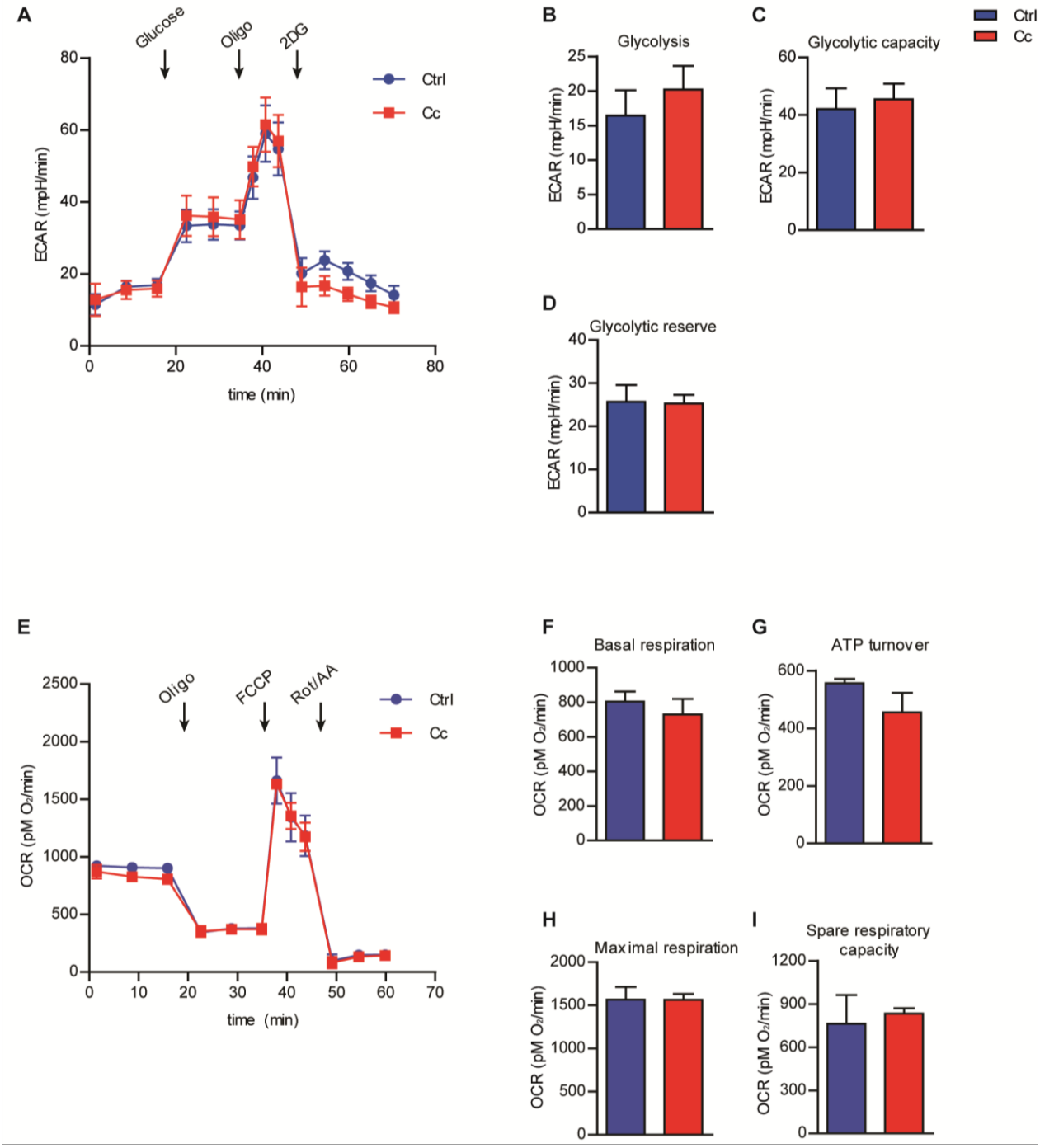

Figure S3 - Effect of Compound C on glycolytic and mitochondrial oxidative phosphorylation profiles in primary neurons. Related to Figure 2.

(**A-I**) Extracellular acidification rate (ECAR, A) and oxygen consumption rate (OCR, E) measured using the Seahorse technology in the presence or absence of the AMPK inhibitor Compound C (Cc, 10 μM). (A) ECAR profile is monitored under basal conditions and upon the sequential injection of saturating concentration of glucose, Oligo and 2DG as indicated by arrows. (E) OCR profile monitored under basal condition and following the sequential injection of Oligo, FCCP, and Rot/AA as indicated by the arrows. ECAR and OCR are indicators of glycolysis and mitochondrial respiration, respectively. (B) Basal glycolysis, (C) glycolytic capacity, and (D) spare glycolytic reserve expressed as mpH/min. (F) Basal respiration, (G) ATP turnover stimulation, (H) maximal respiration, and (I) spare respiratory capacity expressed as pM O_2/min. Results are representative of at least 3 independent experiments.

Results show mean ± SD. One-way ANOVA (B-D, F-I) followed by Bonferroni's post-test were used for evaluation of statistical significance. * $p < 0.05$, ** $p < 0.01$, *** $p < 0.001$.

Figure S4

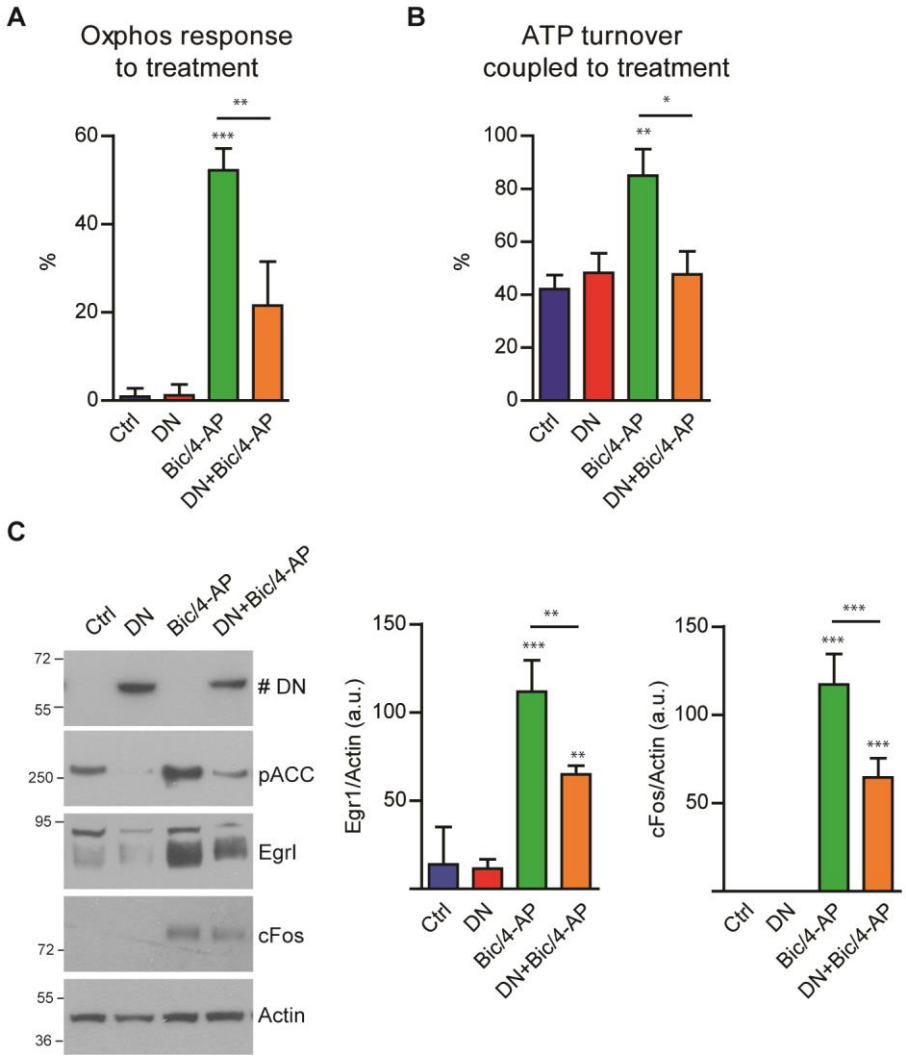

Figure S4 – AMPK inhibition using a dominant negative construct repress the metabolic response to SA and the expression of IEGs. Related to Figure 2 and Figure 4.

(**A-B**) OCR response to treatment (A) and ATP turnover after treatment (B) were evaluated using the Seahorse technology in primary neurons expressing a dominant negative (DN) form of AMPK. Results are expressed as percentage of the first respiration point (n=3). (**C**) Immunoblotting with anti-myc (# DN labels the overexpressed DN-AMPK construct), Egrl, cFos, and Actin in lysates obtained from 15 DIV neurons stimulated with Bic/4-AP for 2 hr, 4 days after infection with DN-AMPK. Results are representative of 3 experiments. Quantification of WB showing the expression of the IEGs Egrl and cFos (n=3).

Results show mean ± SD. One-way ANOVA followed by Bonferroni's post-test was used for evaluation of statistical significance. * $p < 0.05$, ** $p < 0.01$, *** $p < 0.001$.

Figure S5

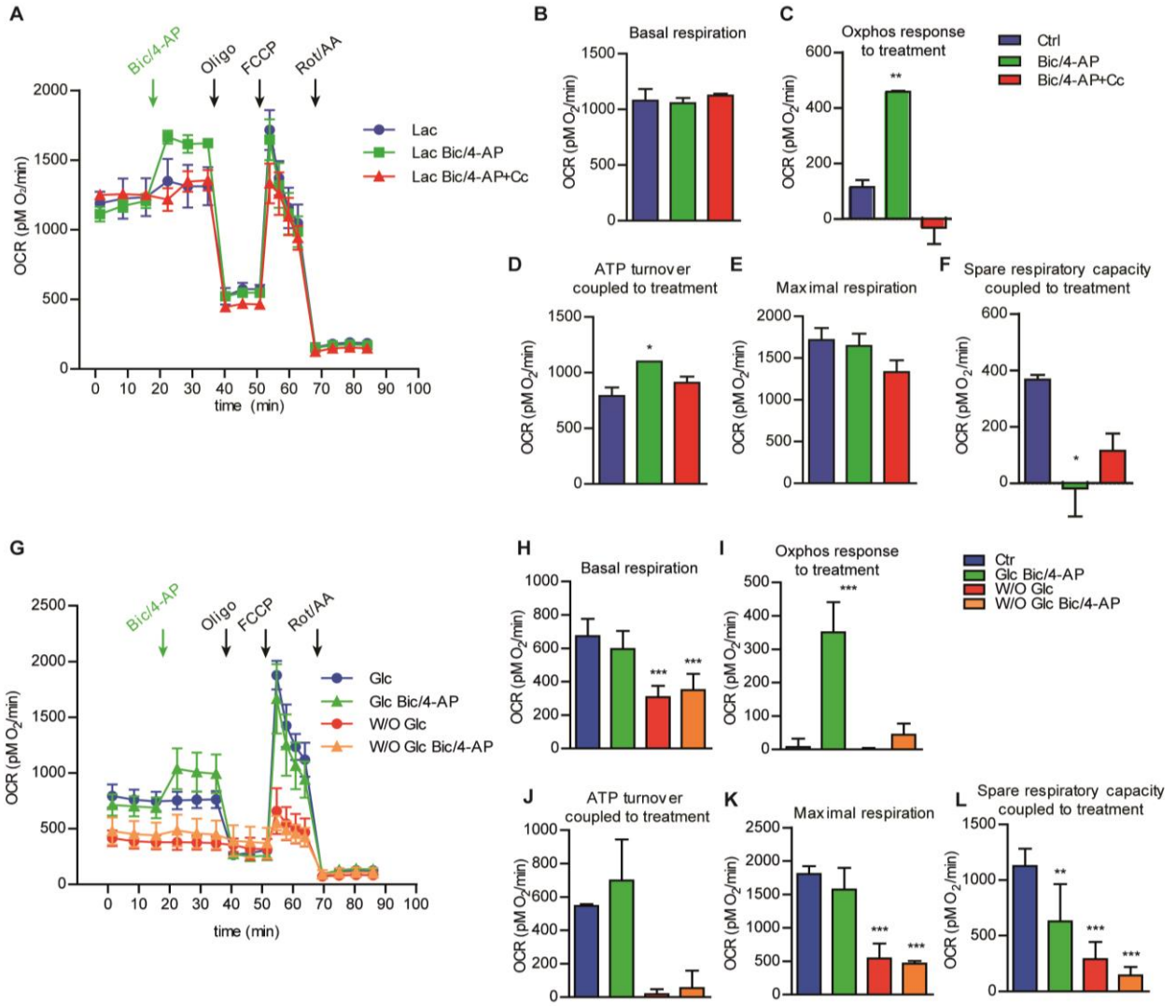

Figure S5 – Utilization of mitochondrial alternative substrates by primary neurons in response to SA. Related to Figure 2 and Figure 3.

(**A**) Oxygen consumption rate (OCR) measured using the Seahorse technology after Bic/4-AP stimulation (green arrows) in the presence or absence of L-Lactate (Lac, 10 mM). OCR profile was monitored under basal conditions and following the sequential injection of assay medium, in Ctrl group, or Bic/4-AP, in the stimulated groups, Oligo, FCCP, and Rot/AA as indicated by the arrows. (**B-F**) Basal respiration (B), oxphos response to treatment (C), ATP turnover after treatment (D), maximal respiration (E), and spare respiratory capacity after treatment expressed as pM O_2/min (F). (**G-L**) Oxygen consumption rate (OCR, G) measured using the Seahorse technology after Bic/4-AP stimulation (green arrows) in the presence (Glc, 10 mM) or

absence (W/O Glc) of glucose. OCR profile was monitored under basal conditions and following the sequential injection of assay medium, in Ctrl group, or Bic/4-AP, in the stimulated groups, Oligo, FCCP, Rot/AA as indicated by the arrows. (H) Basal respiration, (I) oxphos response to treatment, (J) ATP turnover after treatment, (K) maximal respiration, and (L) spare respiratory capacity after treatment expressed as pM O_2/min.

Results are representative of at least 3 independent experiments and show mean ± SD. One-way ANOVA followed by Bonferroni's post-test was used for evaluation of statistical significance. * $p < 0.05$, ** $p < 0.01$, *** $p < 0.001$.

Figure S6

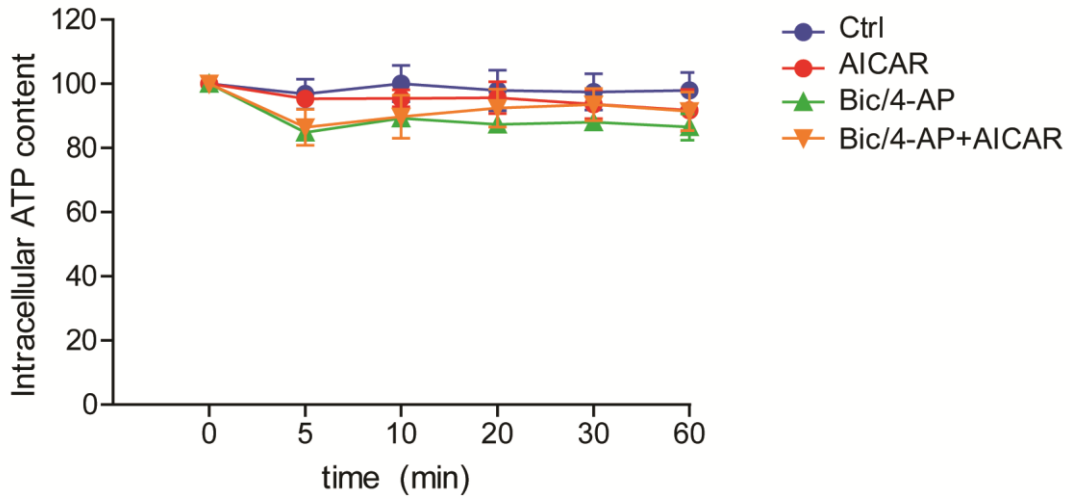

Figure S6 – Intracellular ATP levels following Bic/4-AP stimulation in AICAR pre-treated neurons. Related to Figure 5.

Intracellular ATP levels in neurons pre-treated or not with AICAR (24h, 1mM) and stimulated or not with Bic/4-AP for the indicated times (n=3-4). Results show mean ± SD, values are expressed as percentage of ATP at time 0.

Figure S7

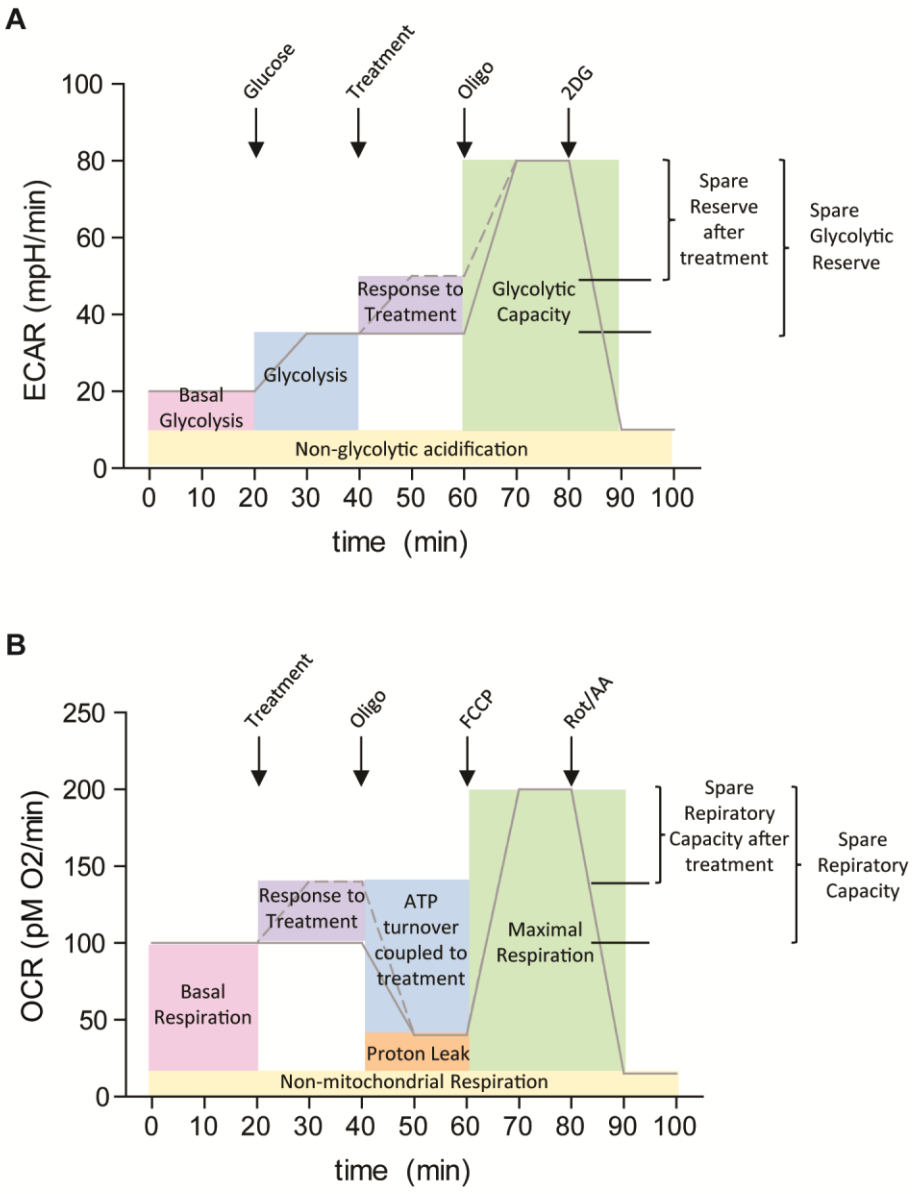

Figure S7 – Schematic representation of metabolic parameters calculated via the Seahorse assay. Related to Figure 2, Figure 5, Figure S3, Figure S4 and Figure S5.

Schematic representation of glycolytic and mitochondrial respiration profile obtained using Seahorse XFe24 respirometry and corresponding metabolic parameters. (**A**) The extracellular acidification rate (ECAR in mpH/min), reflects the intracellular glycolytic flux. Glycolytic flux is monitored in basal conditions as well as during the sequential injection of saturating glucose, treatment, oligomycin (Oligo) and 2-deoxy-D-deoxyglucose (2DG), as indicated by arrows. Glycolysis is calculated as the ECAR value difference before and after glucose injection. Response to Treatment is the maximal ECAR difference before and after

treatment injection. Glycolytic Capacity is calculated as the difference in ECAR between the Non-glycolytic acidification, induced by 2DG injection, and the maximal ECAR value after Oligo injection. Spare glycolytic Reserve is the ECAR difference between Glycolytic Capacity and Glycolysis. Spare Reserve after treatment is the difference between Glycolytic Capacity and Response to Treatment. (**B**) Mitochondrial respiration is expressed in oxygen consumption rate (OCR in pMO_2/min). Mitochondrial respiration is monitored in basal condition as well as during the sequential injection of treatment, oligomycin (Oligo), FCCP and rotenone/antimycin A (Rot/AA). Basal Respiration is obtained as the difference of between the respiration of unstimulated cell, at the beginning of the test, and the OCR value after Rot/AA injection (Non-mitochondrial Respiration). Response to treatment is calculated as the maximal OCR increase in response to treatment injection compared to the OCR at Basal Respiration. ATP turnover after treatment is the difference between the maximal OCR at response to Treatment and minimal OCR value after Oligo injection. Proton leak is difference between the lower OCR value after Oligo injection and Non-mitochondrial respiration. Maximal Respiration is the difference in OCR between the maximal OCR value after FCCP injection and the Non-mitochondrial respiration that is obtained after Rot/AA injection. Spare Respiratory Capacity is the OCR difference between the Maximal Respiration and the Basal Respiration. Spare Respiratory Capacity after treatment is calculated as the difference between the Maximal Respiration and the maximal Response to Treatment.

Transparent Methods

Chemicals and reagents / antibodies

Oligomycin, Carbonyl cyanide-4-(trifluoromethoxy)phenylhydrazone (FCCP), Antimycin A (AA), Rotenone (Rot), 4-Amynopyridine (4-AP), L-Lactate (Lac), iodoacetate and sodium pyruvate (NaPyr) were purchased from Sigma, 2-deoxy-D-glucose (2DG) from Acros, Compound C (Cc) from Santa Cruz, Bicuculline (Bic), MK-801, NBQX, STO-609, N1-(β-D-Ribofuranosyl)-5-aminoimidazole-4-carboxamide (AICAR) and Metformine from Tocris, Glucose 20% solution was purchased from Invitrogen. Antibodies directed against AMPKα, ACC, phospho-Ser^{79}ACC, ERK1/2, phospho-Thr^{202}/Tyr^{204}ERK1/2, phospho-Thr^{581}MSK, phospho-Thr^{380}p90RSK and phospho-Ser^{133}CREB were obtained from Cell Signaling technology. Anti phospho-Thr^{172}AMPKα, Arc, cFos, and EgrI antibodies were from Santa-cruz. Anti-Actin antibody was from BD Transduction Laboratory.

Animals

All animal experiments were performed according to procedures approved by the local Animal Ethical Committee following European standards for the care and use of laboratory animals (agreement APAFIS#4689-2016032315498524 v5 from CEEA75, Lille, France).

Surgical procedures and injections

Three-month-old male C57BL/6J mice were obtained from the Jackson Laboratory. Bilateral hippocampal surgeries were performed as described by Brouillette et al (Brouillette et al., 2012). Briefly, bilateral cannulae (328OPD-2.8/Spc with a removable dummy wire; Plastics One) were stereotaxically implanted into the hippocampus (coordinates with respect to bregma: -2.2 mm anteroposterior [AP], +/- 1.4 mm mediolateral [ML], -2.1 mm dorsoventral [DV], according to the Paxinos and Franklin mouse brain atlas) in anesthetized mice (100 mg/kg of ketamine and 10 mg/kg of xylazine, i.p.). After surgery, the animals recovered for 10 days before undergoing any procedures. After 10 days of recovery, awake and freely moving mice were injected once with 2 µl of Compound C or an equal volume of vehicle buffer at a rate of 0.25 µl/min via cannulae PE50 tubing (Plastics One) connected to a 10 µL Hamilton syringe pump system (KDS310; KD Scientific). The cannulae was capped to prevent reflux of the injected solution.

Inhibitory avoidance

Ten days after the surgery, mice underwent the inhibitory avoidance (IA) paradigm. Control mice (Saline) were injected with saline solution (0.9 % NaCl) while the treated mice were injected with Compound C (2 µl at 100 µM in saline) 20 min before running the acquisition test (Acq). The IA apparatus consisted in a rectangular shaped box that is divided into a safe illuminated compartment and a dark shock compartment. During the Acq session, each mouse was placed in the safe compartment and allowed to access the dark chamber where a brief foot shock (0.3 mA, 2 s) was delivered. The mouse was left in the dark compartment for one minute, before being replaced in its home cage. Latency to enter the shock compartment was taken as a measure of acquisition (Acq). 24 hr later, a retention test (Test 1) was run. In this phase, each mouse was placed in the light chamber and the latency to enter the dark compartment was recorded, however no foot shock was delivered when the mouse entered the dark chamber. A second test was run 6 days after the acquisition test (Test 2) in order to assess memory retention. To verify the ability of the injected mice to make new long term memory, each injected mouse underwent a second acquisition test 7 days after the first one (Retraining), and retention was tested 24 hr after (Test 3).

Extracellular long-term recordings in the CA1-region of the hippocampus

Mice were killed by cervical dislocation and hippocampal slices prepared from the dorsal area of the right hippocampus as reported previously (Ahmed et al., 2015; Denayer et al., 2008). In brief, the right hippocampus was rapidly dissected out into cold (4^{o}C) artificial cerebrospinal fluid (ACSF), saturated with carbogen (95% O_2/5% CO_2). ACSF consisted of 124 NaCl, 4.9 KCl, 25.6 $NaCO_3$, 1.20 KH_2PO_4, 2.0 $CaCl_2$, 2.0 $MgSO_4$, and 10.0 glucose (in mM), adjusted to pH 7.4. Transverse slices (400 µm thick) were prepared from the dorsal area of the right hippocampus with a tissue chopper and placed into a submerged-type chamber, where they were kept at 32^{o}C and continuously perfused with ACSF at a flow-rate of 2.2 ml/min. After 90 min incubation, one slice was arbitrarily selected and a custom-made tungsten electrode was placed in CA1 stratum radiatum for stimulation in constant current mode. For recording of field excitatory postsynaptic potentials (fEPSPs), a glass electrode (filled with ACSF, 3-7 MΩ resistance) was placed in the stratum radiatum. The time course of the field EPSP (fEPSP) was measured as the descending slope function for all sets of experiments. After a further hour of incubation, input/output curves were established and the stimulation strength was adjusted to elicit a fEPSP-slope of 35% of the maximum and was kept constant throughout the experiment. During baseline recording, three single stimuli (0.1 ms pulse width; 10 s interval) were measured every 5 min and averaged. A robust LTP was induced by three theta

burst stimuli (TBS), separated by 10 min. Compound c (Cc) was applied from 30 minutes prior to until 30 min after the first TBS. To allow for direct comparisons all experiments were interleaved between the experimental and control group. Intergroup differences in LTP were examined using ANOVA with repeated measures (RM-ANOVA, SPSS 19). For intragroup comparisons, Wilcoxon's matched-pairs signed-rank test was employed (SPSS 19). Group differences at single time points were tested using the Welch-test.

Primary Neuronal Culture

Primary neurons were prepared as previously described (Domise et al., 2016). Briefly, foetuses at stage E18.5 were obtained from pregnant C57BL/6J wild-type female mice (The Jackson Laboratory). Forebrains were dissected in ice-cold dissection medium composed of Hanks' balanced salt solution (HBSS) (Invitrogen) supplemented with 0.5 % w/v D-glucose (Sigma) and 25 mM Hepes (Invitrogen). Neurons were dissociated and isolated in ice-cold dissection medium containing 0.01 % w/v papain (Sigma), 0.1 % w/v dispase (Sigma), and 0.01 % w/v DNaseI (Roche) and by incubation at 37 °C for 15 min. Cells were spun down at 220 x g for 5 min at 4°C, resuspended in Neurobasal medium supplemented with 2% B27, 1 mM NaPyr, 100 units/ml penicillin, 100 µg/ml streptomycin, 2 mM Glutamax (Invitrogen), and plated at a density of $6*10^6$ cells/plate. Fresh medium was added every 3 days (1:3 of starting volume). Cells were then treated and collected between DIV 14-17.

Construct and production of lentiviral vectors

N-terminally myc-tagged wild-type (wt) and K45R mutated AMPKα2 rat sequences were subcloned from Addgene plasmids 15991 and 15992 (Mu et al., 2001) into pENTR/D backbone using the In-Fusion HD cloning kit (Clontech) with the following primers: Fwd: 5'-CACCATGGTGCGGGGTTCTCAT and Rev-Trunc: 5'-GTCACCCTAGTATAAACTGTTCATCAC for the wtAMPKα2 and Rev: 5'-TCAACGGGCTAAAGCAGTGATA for the K45R-AMPKα2 to obtain respectively a constitutive active (CA) truncated form of AMPK ending at position 312, the AMPKα2(1-312)-pENTR/D, and a kinase dead dominant negative (DN) form of AMPK, the AMPKα2K45R-pENTR/D. Subsequently, pENTR/D vectors were recombined with SIN-PGK-cPPT-RFA-WHV lentiviral vectors using the Gateway LR Clonase II enzyme (Thermo Fisher) to obtain AMPKα2(1-312)-pLenti and AMPKα2K45R-pLenti constructs. The production of lentiviral vectors (LV) batches was as previously described (Caillierez et al., 2013). Primary neurons were infected with LV at 10 DIV and were used for experiments 4 days after LV infections.

Intracellular ATP quantification

Intracellular ATP content was quantified using the Dual-Glo® Luciferase Assay System (Promega), according to the supplier's instructions. Briefly, after treatments, primary neurons were incubated with the Dual- Glo® substrate for 10 min at RT before assessing luciferase activity using Spectramax® i3 (Molecular Devices).

Phospho-Kinase array

For the phospho-kinase assay, the array membranes were incubated with cell lysates (250 µg of total proteins per array) and subsequently processed according to the manufacturer's instructions (R&D Systems).

Seahorse assay

For Seahorse XFe24 respirometry assay, 100,000 neuronal cells were seeded in each well. The assay medium was composed of Dulbecco's Modified Eagle Medium base (DMEM, D-5030 Sigma) supplemented with 2 mM L-Glutamine (Invitrogen), 1.85 g/l NaCl (VWR), 3 mg/l Phenol Red (Sigma) and adjusted to pH 7.3+/-0.05. For each assay, cells were rinsed with the assay medium before being pre-incubated at 37°C without CO_2 20 min prior the reading. For the glycolytic test, the extracellular acidification rate (ECAR in mpH/min) was monitored during basal condition (the mixing 2:30 min, waiting 2:00 min, reading 2:30 min cycle was repeated three times) and upon the sequential addition of saturating concentration of Glucose (10 mM) (the mixing 2:30 min, waiting 2:00 min, reading 2:30 min cycle was repeated 3 times), followed by Bic/4-AP (50 µM/2.5 mM) (the mixing 1:00 min, waiting 1:00 min, reading 2:30 min cycle was repeated five times), oligomycin (Oligo 1 µM) (the mixing 2:30 min, waiting 2:00 min, reading 2:30min cycle was repeated two times), and 2DG (150 mM) (the mixing 2:30 min, waiting 2:00 min, reading 2:30 min cycle was repeated two times). Glycolysis was expressed as ECAR increase after glucose addition. The glycolytic response to Bic/4-AP was calculated as the ECAR difference before and after the injection of Bic/4-AP, glycolytic capacity was calculated as the maximum ECAR reached following oligomycin injection when compared to basal conditions before glucose injection, glycolytic reserve as the difference between ECAR increase after oligomycin addition and upon glucose injection. The spare glycolytic reserve after Bic/4-AP injection was calculated as the percentage of the glycolytic reserve spared upon response to Bic/4-AP

treatment. In the mitochondrial stress test, the oxygen consumption rate (OCR in pMO_2/min) was monitored during the basal condition (the mixing 1:30 min, waiting 2:00 min, reading 3:00 min cycle was repeated three times) and after the subsequent injection of Bic/4-AP (50 µM/2.5 mM) (the mixing 1:30 min, waiting 2:00 min, reading 2:00 min cycle was repeated three times), oligomycin (Oligo, 1 µM) (the mixing 1:20min, waiting 1:20min, reading 2:00min cycle was repeated three times), FCCP (0.5 µM) (the mixing 0:20 min, waiting 0:00 min, reading 2:00 min cycle was repeated four times), Rotenone/Antimycin A (Rot/AA 1 µM/1 µM) (the mixing 1:20 min, waiting 1:20 min, reading 2:00 min cycle was repeated three times). For mitochondrial stress test, the assay medium was supplemented with glucose (10 mM), or L-Lactate (10 mM), or NaPyr (10 mM), as specified, before the pre-incubation without CO_2. Basal respiration was expressed as the difference in OCR before Bic/4-AP and after Rot/AA injection. The oxphos response to Bic/4-AP was expressed as the increase of OCR before and after Bic/4-AP addition. ATP turnover after Bic/4-AP treatment was calculated as the OCR difference before and after oligomycin injection. Maximal respiration was calculated as the OCR increase after FCCP compared to OCR upon Rot/AA injection, while spare respiratory capacity was expressed as the increase in OCR after FCCP when compared to basal respiration OCR level. Spare respiratory capacity after Bic/4-AP treatment was calculated as the percentage of mitochondrial OCR spare respiratory capacity after Bic/4-AP injection. Graphical explanation of each of the measurements is depicted in Figure S7. The pH of the drug solutions were adjusted to pH 7.3+/-0.05 prior to their use.

Metabolomics analysis

Five hundred thousand neurons were supplemented with media containing uniformly labelled ^{13}C-glucose (25 mM) for 30 min. Cells were rinsed with ice-cold 0.9% NaCl solution and metabolites were extracted by adding 250 µl of a 50-30-20 solution (methanol-acetonitrile-10 mM tris HCl pH 9.4) to the cells. Plates were then incubated for 2-3 min on ice. Cells were scraped and transferred to an eppendorf tube before centrifugation at 20,000 x g for 10 min at 4°C, supernatants were then transferred to a fresh tube and stored at -80°C. Separation of metabolites prior to Mass Spectrometry (MS) measurement was performed using a Dionex UltiMate 3000 LC System (Thermo Scientific) coupled to a Q Exactive Orbitrap mass spectrometer (Thermo Scientific) operating in negative ion mode. Practically, 15 µl of the cellular extract was injected on a C18 column (Aquility UPLC®HSS T3 1.8µm 2.1x100mm) and the following gradient was performed by solvent A (H_2O, 10mM Tributyl-Amine, 15mM acetic acid) and solvent B (100% Methanol). Chromatographic separation was achieved with a flowrate of 0.250ml/min and the following gradient

elution profile: 0min, 0%B; 2min, 0%B; 7min, 37%B; 14min, 41%B; 26min, 100%B; 30min, 100%B; 31min, 0%B; 40min, 0%B. The column was placed at 40°C throughout the analysis. The MS operated both in full scan mode (m/z range: 70-1050) using a spray voltage of 4.9 kV, capillary temperature of 320°C, sheath gas at 50.0, auxiliary gas at 10.0. The AGC target was set at 3e6 using a resolution of 140.000, with a maximum IT fill time of 512 ms. Data collection was performed using the Xcalibur software (Thermo Scientific).

Western blot (WB)

For WB analysis, proteins from total cell lysates were separated in 8-16% Tris-Glycine gradient gels and transferred to nitrocellulose membranes. Membranes were then blocked in 5% fat-free milk in TBS-0.01% Tween-20, and incubated with specific primary antibodies overnight at 4 °C. Proteins were thereafter detected via the use of HRP-conjugated secondary antibodies and ECL detection system (ThermoFisher Scientific).

Statistical analysis

All statistical analyses were performed using GraphPad Prism (Prism 5.0d, GraphPad Software Inc, La Jolla, CA, USA).

References

Ahmed, T., Blum, D., Burnouf, S., Demeyer, D., Buee-Scherrer, V., D'Hooge, R., Buee, L., and Balschun, D. (2015). Rescue of impaired late-phase long-term depression in a tau transgenic mouse model. Neurobiology of aging *36*, 730-739.

Brouillette, J., Caillierez, R., Zommer, N., Alves-Pires, C., Benilova, I., Blum, D., De Strooper, B., and Buee, L. (2012). Neurotoxicity and memory deficits induced by soluble low-molecular-weight amyloid-beta1-42 oligomers are revealed in vivo by using a novel animal model. The Journal of neuroscience : the official journal of the Society for Neuroscience *32*, 7852-7861.

Caillierez, R., Begard, S., Lecolle, K., Deramecourt, V., Zommer, N., Dujardin, S., Loyens, A., Dufour, N., Auregan, G., Winderickx, J.*, et al.* (2013). Lentiviral delivery of the human wild-type tau protein mediates a slow and progressive neurodegenerative tau pathology in the rat brain. Molecular therapy : the journal of the American Society of Gene Therapy *21*, 1358-1368.

Denayer, E., Ahmed, T., Brems, H., Van Woerden, G., Borgesius, N.Z., Callaerts-Vegh, Z., Yoshimura, A., Hartmann, D., Elgersma, Y., D'Hooge, R.*, et al.* (2008). Spred1 is required for synaptic plasticity and hippocampus-dependent learning. The Journal of neuroscience : the official journal of the Society for Neuroscience *28*, 14443-14449.

Domise, M., Didier, S., Marinangeli, C., Zhao, H., Chandakkar, P., Buee, L., Viollet, B., Davies, P., Marambaud, P., and Vingtdeux, V. (2016). AMP-activated protein kinase modulates tau phosphorylation and tau pathology in vivo. Scientific reports *6*, 26758.

Mu, J., Brozinick, J.T., Jr., Valladares, O., Bucan, M., and Birnbaum, M.J. (2001). A role for AMP-activated protein kinase in contraction- and hypoxia-regulated glucose transport in skeletal muscle. Molecular cell *7*, 1085-1094.